Layering Instability in a Confined Suspension Flow

M. Zurita-Gotor, J. Bławzdziewicz, and E. Wajnryb

Phys. Rev. Lett. **108**, 068301 — Published 10 February 2012

DOI: 10.1103/PhysRevLett.108.068301

Layering instability in a confined suspension flow

M. Zurita-Gotor,[1] J. Bławzdziewicz,[2] and E. Wajnryb[3]

[1] *Departmento de Ingeniería Aeroespacial y Mecánica de Fluidos, Universidad de Sevilla, Sevilla 41092, Spain*
[2] *Department of Mechanical Engineering, Texas Tech University, Lubbock, Texas 79409, USA*
[3] *Institute of Fundamental Technological Research, Warsaw, Polish Academy of Sciences*

(Dated: December 12, 2011)

We have shown [J. Fluid Mech. **592**, 447 (2007)] that swapping (reversing) trajectories in confined suspension flows prevent collisions between particles approaching each other in adjacent streamlines. Here we demonstrate that by inducing layering this hydrodynamic mechanism changes the microstructure of suspensions in a confined Couette flow. Layers occur either in the near-wall regions or span the whole channel width, depending on the strength of the swapping-trajectory effect. While our theory focuses on dilute suspensions, we postulate that this new hydrodynamic mechanism controls formation of a layered microstructure in a wide range of densities.

PACS numbers: xxxx

Confined particulate flows have important applications in microfabrication, microfluidics and biotechnology. Recent studies have shown complex nonlinear microstructural evolution [1–8], strikingly different than the behavior with no confining walls. Confinement imposes geometrical constraints on particle motion and also gives rise to purely hydrodynamic mechanisms. Geometry-driven phenomena have been extensively studied (e.g., ordered structures in tightly confined dense suspensions and emulsions [1]), but hydrodynamic mechanisms that are wall-induced have only recently been at the center of attention. So far the most thoroughly investigated hydrodynamic confinement phenomenon is the fluid backflow produced by particle motion, e.g. in linear conduits [9, 10], and in parallel-wall channels [4, 11]. The backflow gives rise to the anomalous sign of the mutual diffusion coefficient for Brownian spheres [4, 11], wave propagation in drop or particle trains [5, 6, 8], and unusual stability of a square particle lattice [6, 8].

Here we demonstrate that the evolution of suspension microstructure depends on the swapping (reversing) trajectory effect [12, 13]. This proposed wall-induced hydrodynamic mechanism prevents collisions of particles in adjacent streamlines in a confined Couette flow. As a result, a uniform suspension microstructure is destabilized, leading to the formation of particle layers (cf., Figs. 1 and 2). Layered microstructure arises spontaneously in confined flows, even at moderate particle concentrations. It has recently been observed in computer simulations and experiments [2, 3] (also in movies A1–A4 in Supplemental Materials [14]). We describe the key hydrodynamic mechanism responsible for this behavior.

We consider a suspension of non-Brownian spherical particles in planar Couette flow of shear rate $\dot\gamma$, under creeping-flow conditions [cf., Fig. 1(a)]. The particles have finite roughness, which is modeled by a very steep, short-range repulsive potential of the range $d_r = d+\epsilon$ [14] (where d is the hydrodynamic diameter) to mimic contacts between roughness asperities. These direct particle

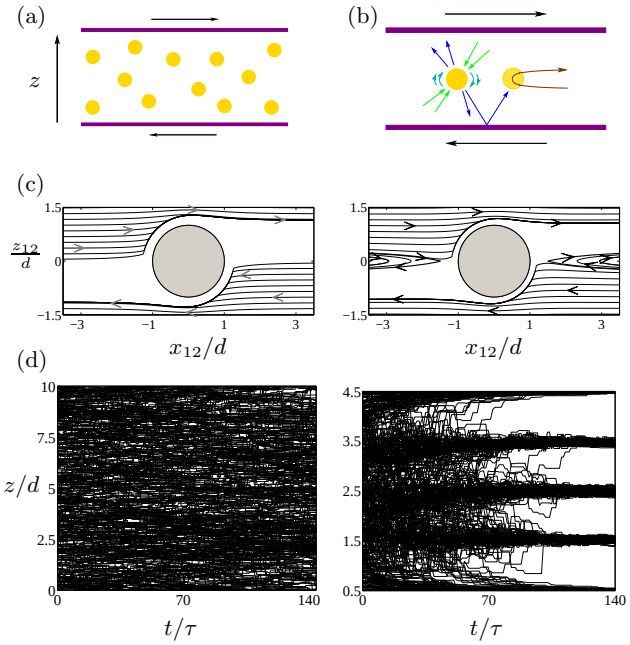

FIG. 1. Wall-induced layering. (a) Suspension geometry. (b) Swapping-trajectory (ST) effect: the flow scattered from the walls produces lift causing the reversal of particle motion. (c) Relative particle trajectories in two systems: unconfined (left) and confined with the ST region (right). (d) Time evolution of transverse particle positions z in suspension: unconfined (left) and confined (right). Time is normalized by the characteristic time between collisions $\tau = 1/(n_0\dot\gamma d^3)$. (Color online)

contacts remove the Stokes-flow symmetry of binary collisions, producing finite transverse particle displacements [15], as illustrated in Fig. 1(c).

Our analysis is focused on the dilute-suspension limit. The simulations in Figs. 1 and 2 are performed using the Boltzmann–Monte Carlo (BMC) method, in which the system dynamics is modeled as a sequence of uncorrelated binary collisions [12, 14]. Since particle correlations are important only at higher concentrations, this

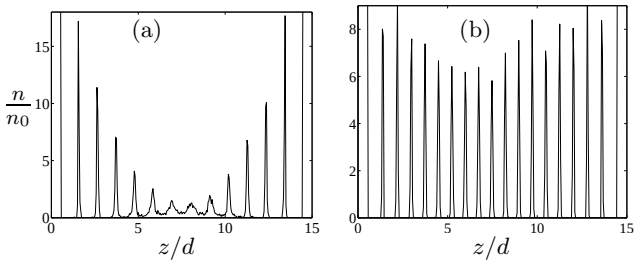

FIG. 2. Suspension microstructure for particles of different roughness in a channel of width $H/d = 15$ at time $t/\tau = 2400$. Density profiles n/n_0 are shown vs transverse position z/d. Roughness range (a) $\epsilon/d = 0.25$; (b) $\epsilon/d = 0.064$.

method is appropriate in the low-concentration regime. We analyze suspensions at low concentrations n_0 to emphasize physical mechanisms involved in the formation of the layered microstructure, but our direct numerical simulations (cf., movies B1-B4 in [14]) show that these mechanisms are present also at higher concentrations.

In the BMC method, the particle distribution is evolved by performing a sequence of uncorrelated collisional steps. In each step, we choose a random pair of particles, simulate their binary collision, and update the cross-streamline particle positions according to the post-collisional displacements [14]. When binary trajectories are accurately evaluated, taking into account the hydrodynamic interactions (HI) in the wall presence [11, 14], we refer to this description as BMC-HI. To highlight the role of topological features of pair trajectories without incurring the large computational cost of evaluation of HI, we use two simplified collision models M2 and M3, described below. Figures 1 and 2 were obtained using BMC-HI, and Figs. 3–6 correspond to models M2 and M3.

Figure 1(d) demonstrates that a suspension confined between two parallel walls develops a well-defined layered structure (after about 20 collisions per particle), while the unconfined system remains uniform. Fig. 2 illustrates a strong dependence of the layered structure on the range ϵ of non-hydrodynamic interparticle interactions.

We argue that the observed layering behavior stems from the swapping-trajectory (ST) effect that causes approaching particles to reverse their motion, and avoid collision (cf., movie B1 in [14]). As depicted in Fig. 1(b), the ST domain results from wall-mediated interparticle HI: the wall reflection of the perturbation flow produced by one of the particles pushes the other particle across streamlines of the applied flow toward the fluid moving in the opposite direction [12]. The reversal of the relative particle motion prevents large collisional displacements for particles with a sufficiently small transverse offset [cf., Fig. 2(c)], leading to stabilization of particle layers. This effect is seen in Movie A1 in [14], where random particle collisions drive a confined suspension towards a layered configuration with reduced frequency of particle contacts (also see our additional discussion in Sec. 5 in [14]).

Population-balance equation – To provide a quantitative description of the effect of swapping trajectories on the suspension dynamics we use the population-balance method, where the particle density $n(z)$ (uniform in the flow and vorticity directions x and y) is described by a master equation that accounts for the effect of binary particle collisions on the suspension motion. In the simplest two-dimensional (2D) version (with no y direction), the master equation reads

$$\frac{\partial n\,(z,t)}{\partial t} = \dot\gamma \int_{-\infty}^{\infty} [n(z+\tfrac{1}{2}\Delta-\tfrac{1}{2}\Delta')n(z-\tfrac{1}{2}\Delta-\tfrac{1}{2}\Delta') - n(z)n(z-\Delta)]\,\Delta\, d\Delta, \qquad (1)$$

where Δ and Δ' are the pre-collision and post-collision particle offsets. For simplicity, we assume that the interacting particles undergo symmetric transverse displacements. The first term of the integrand in Eq. (1) corresponds to collisions pushing a particle into position z (moving it from $z+\frac{1}{2}\Delta-\frac{1}{2}\Delta'$), and the second term to collisions displacing a particle from position z. If the initial and final offsets are the same, $\Delta = \Delta'$, the first and second terms of the integrand cancel. In the full three-dimensional (3D) version, an additional integration with respect to the lateral offset Δy is present [14].

Collision models M2 and M3 – Based on the geometry of binary collisions [cf., Fig. 3(a)], we introduce a 2D collision model M2,

$$\Delta' = \begin{cases} -\Delta, & 0 < |\Delta| < \kappa_s, \\ \mathrm{sign}(\Delta)\kappa_c, & \kappa_s < |\Delta| < \kappa_c, \\ \Delta, & \kappa_c < |\Delta| < \infty, \end{cases} \qquad (2)$$

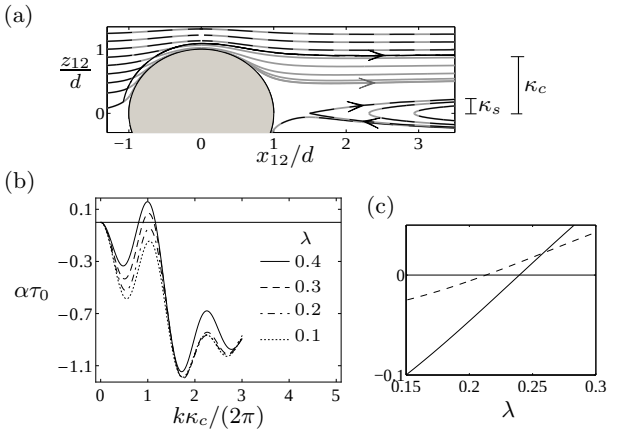

FIG. 3. (a) Pair collisions: relative trajectories for roughness range $\epsilon/d = 9\times10^{-2}$ (dashed lines) and $\epsilon/d = 10^{-3}$ (gray solid). (b) Growth rate α of small harmonic perturbations vs the wavevector k for several values of the swapping ratio λ (as labeled) in model M2. (c) Peak value of α vs swapping ratio λ for model M2 (solid) and M3 (dashed). The growth-rate ratio α is normalized by the characteristic time $\tau_0 = 1/(\dot\gamma n_0 \kappa_c^D)$, where D is the dimensionality of the model.

where κ_s is the swapping range and κ_c collision range. For a collision parameter $|\Delta| < \kappa_s$, swapping leads to the exchange of transverse particle positions, consistent with the results of our hydrodynamic calculations, and the two terms of the integrand in Eq. (1) cancel. For the collision parameter in the range $\kappa_s < |\Delta| < \kappa_c$ there are finite particle displacements contributing to the evolution of the density n. In our 3D model M3 [14], particles on collisional trajectories behave as hard spheres without HI, and in the swapping trajectory region $|\Delta| < \kappa_s$ they exchange their transverse positions z.

Small perturbation analysis – We show that the existence of the swapping region $|\Delta| < \kappa_s$ results in a layering instability, provided that the swapping ratio

$$\lambda = \kappa_s/\kappa_c \tag{3}$$

is sufficiently large. The conditions for a uniform particle distribution n_0 to become unstable can be derived by analyzing small harmonic perturbations $n(z;t) = n_0 + n_1(t)e^{\mathrm{i}kz}$. For the translationally invariant population-balance models M2 and M3, such Fourier modes evolve exponentially, $n_1(t) = n_1(0)e^{\alpha t}$. Figure 3(b) shows that the growth rate $\alpha(k)$ has a peak around $k \approx 2\pi/\kappa_c$. Since the peak value becomes positive at a critical swapping ratio $\lambda = \lambda_c$, the uniform particle distribution is unstable to small perturbations for $\lambda > \lambda_c$, leading to formation of particle layers. Figure 3(b) shows results for M2, but M3 yields a similar behavior. In Fig. 3(c) the peak values of α are plotted vs. the swapping ratio λ (for M2 and M3). For M2 the critical swapping ratio is $\lambda_c = 0.24$, and for M3 $\lambda_c = 0.213$. Our BMC-HI simulations yield the instability in a similar parameter range.

Based on the dynamics of pair collisions (with HI), the swapping ratio (3) can be controlled in two ways. First, the swapping range κ_s can be changed by varying the wall separation H. For example, for a particle pair in the middle of the channel, the dimensionless range κ_s/d varies between 0.27 for $H/d = 5$ and 0.12 for $H/d = 40$ [12]. Second, the swapping ratio can also be controlled by changing particle roughness, because collision range κ_c diminishes with the decreasing roughness amplitude [15], as shown in Fig. 3(a). We thus predict that by decreasing the magnitude of the particle roughness, we can induce formation of a long-range order in a confined suspension under shear. This prediction is confirmed by our BMC-HI simulations (cf., Fig. 2, where $\lambda = 0.163$ for $\epsilon/d = 0.25$ and $\lambda = 0.23$ for $\epsilon/d = 0.064$, based on the mid-channel swapping range $\kappa_s/d = 0.189$).

Near-wall microstructure – Further predictions regarding the wall-induced suspension ordering can be obtained when geometrical constraints that disallow particle–wall overlaps are introduced into the population-balance model (1). Figures 4 and 5 show our results for model M3 with such constraints. We consider a system with a large wall separation $H/\kappa_c = 60$ to emphasize

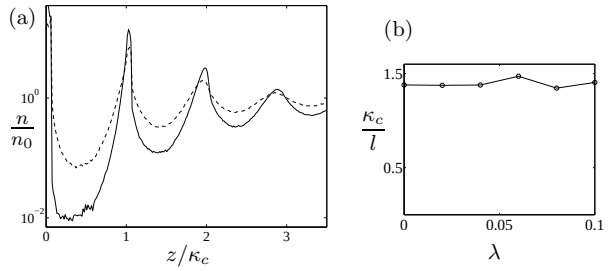

FIG. 4. Long-time near-wall suspension microstructure for subcritical values of swapping ratio λ (model M3) (a) Density profile n/n_0 for $\lambda = 0$ (dashed line) and $\lambda = 0.1$ (solid). (b) inverse correlation length l^{-1} vs λ.

two important regimes of suspension behavior: subcritical (Fig. 4) and supercritical (Fig. 5). In both regimes we observe formation of a wall-induced layered order, but the evolution and extent of the layered microstructure is regime-specific. For subcritical values of the swapping ratio (3), only the near-wall domain is affected, whereas for supercritical values the layered structure propagates from the wall into the bulk of the suspension.

Subcritical regime – Figure 4(a) shows the subcritical microstructure for $\lambda = 0$ (no swapping) and $\lambda = 0.1$ (significant swapping). In both cases several particle layers form near the wall. The correlation length l of this local layered structure is insensitive to the value of λ [cf., Fig. 4(b)], but for $\lambda = 0$ the layers are fuzzy, with many particles between the density peaks, and for $\lambda = 0.1$ the

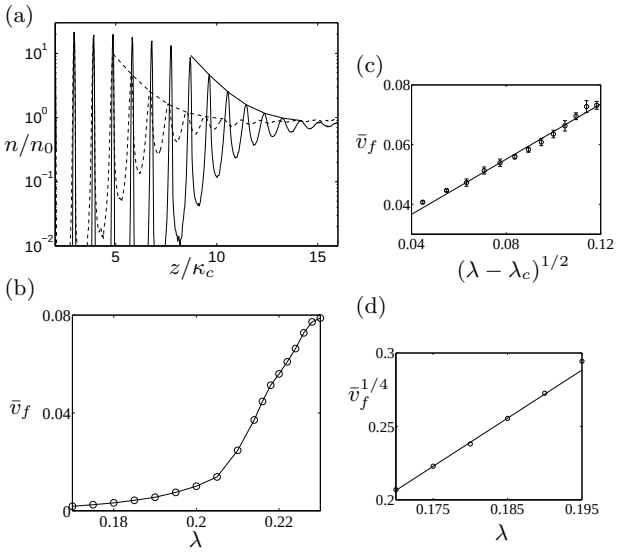

FIG. 5. Near-wall suspension microstructure for supercritical values of swapping ratio λ (model M3). (a) Density profile at times $t_1/\tau_0 = 1250$ (dashed line) and $t_2/\tau_0 = 2500$ (solid line) for swapping ratio $\lambda = 0.18$ and channel width $H/d = 60$. Characteristic time $\tau_0 = 1/\left(n_0\dot{\gamma}\kappa_c^3\right)$. (b) Normalized propagation velocity $\bar{v}_f = v_f\tau_0/\kappa_c$. Near critical scaling behavior of $\bar{v}_f$ for two cases: (c) $\lambda \gtrsim \lambda_c$, and (d) $\lambda \gtrsim \lambda_w$.

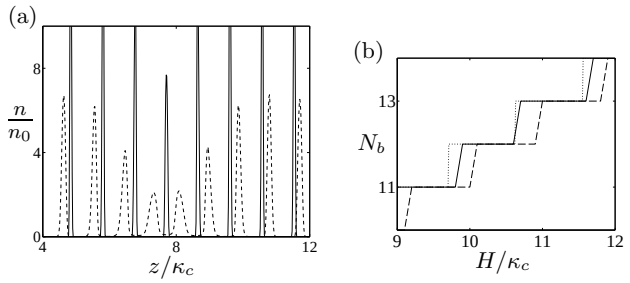

FIG. 6. Layer restructuring for supercritical swapping ratio $\lambda = 0.24$ (model M3). (a) Merging of two central layers when the width is incommensurate $H/\kappa_c = 15.4$; intermediate time (dashed line), long time (solid). (b) Number of layers vs normalized channel width: maximal number during evolution (solid); steady state (dashed); estimate based on the wavelength of the most unstable Fourier mode (dotted).

layers are sharp. The ST mechanism influences the form but not the extent of the subcritical microstructure.

Supercritical regime – In the supercritical regime (cf. Fig. 5) the wall-induced microstructure propagates from the wall with velocity v_f, forming a growing number of particle layers, as shown in Fig. 5(a). In a fully developed microstructure the layers are well separated, and particle jumps between layers are rare [cf., Fig. 1(d)]. The propagation velocity v_f of the layered structure in this regime [cf. Fig. 5(b)] is an increasing function of λ, with two distinct dynamical domains. For $\lambda > \lambda_c$ (suspension unstable to small perturbations), v_f rapidly increases with the swapping ratio, showing a power law critical behavior $v_f \sim (\lambda - \lambda_c)^{1/2}$ [cf. Fig. 5(c)]. In the domain $\lambda_w < \lambda < \lambda_c$ the suspension is stable to small perturbations, but unstable to the *large perturbation* caused by the wall. In this regime, the data can be well fitted to the power law $v_f \sim (\lambda - \lambda_w)^\beta$ with $\lambda_w \approx 0.11$ and $\beta \approx 4$ [cf. Fig. 5(d)]. Due to the large value of the exponent β, the propagation velocity v_f is practically zero for $\lambda \lesssim 0.16$.

The layer separation in the propagating microstructural fronts may be incommensurate with the wall separation. In such cases the two mid-channel layers merge, and after restructuring the width of the density peaks decreases [cf., Fig. 6(a)]. The number of layers agrees well with our prediction based on the wavelength of the most unstable Fourier mode [cf. Fig. 6(b)].

Conclusions – The ST mechanism significantly alters the suspension microstructure in a confined Couette flow by inducing layering. Previously (solving a long-standing paradox [16]), we have demonstrated that swapping trajectories cause the anomalous enhancement of hydrodynamic diffusion, and that they stabilize particle chains in microfluidic channels [12]. The layering behavior identified here adds to the growing evidence that a seemingly subtle ST effect has far-reaching consequences in confined particulate flows. Our direct numerical simulations indicate that swapping trajectories significantly influence a variety of confined systems, including suspensions at higher concentrations [14] and flow-driven particle monolayers [8] (which have a similar structure to the layers observed experimentally in [3]). In suspensions with nonzero inertial forces [17] and in viscoelastic fluids, swapping (reversing) trajectories occur even without confinement, so the ST mechanism is likely to affect suspension microstructure in such flows.

Wall-induced layering instabilities have been observed also for thermal systems. A transition between a short-range and non-local long-range layered microstructure has been predicted using a dynamic density-functional theory for a suspension of Brownian particles [18]. Similar layering was seen in computer simulations of confined molecular systems under shear [19]. It seems that such systems have an important common feature: development of inhomogeneous microstructure is associated with a decrease in collisional frequency when layers form.

Finally, we note that the suspension behavior described in our study significantly differs from the dynamics of a dilute gas. In a gas, binary collisions always produce a homogeneous equilibrium state, according to Boltzmann's H-theorem. By analogy, it is usually assumed that binary collisions in suspension flows always lead to a diffusive behavior that results in relaxation of density fluctuations. Here we report that *uncorrelated binary collisions* produce inhomogeneous layered microstructure.

We acknowledge financial support by NSF grant CBET 1059745 (JB), Ministerio de Innovación y Ciencia grant RYC-2008-03650 (MZG), and Polish Ministry of Science and Higher Education grant N N501 156538 (EW).

[1] T. Thorsen, R. W. Roberts, F. H. Arnold, and S. R. Quake, Phys. Rev. Lett. **86**, 4163 (2001); I. Cohen, T. G. Mason, and D. A. Weitz, *ibid.* **93**, 046001 (2004).
[2] A. Komnik, J. Harting, and H. Herrman, J. Stat. Mech.: Theory Exp., P12003(2004); K. Yeo and M. Maxey, Phys. Rev. E **81**, 051502 (2010); X. Cheng, X. Xu, S. A. Rice, A. R. Dinner, and C. Itai, PNAS **xx**, xxx (2011).
[3] X. Cheng, J. H. McCoy, J. N. Israelachvili, and I. Cohen, Science **333**, 1276 (2011).
[4] B. Cui, H. Diamant, B. Lin, and S. A. Rice, Phys. Rev. Lett. **92**, 258301 (2004).
[5] T. Beatus, T. Tlusty, and R. Bar-Ziv, Nature Physics **2**, 743 (2006); T. Beatus, R. Bar-Ziv, and T. Tlusty, Phys. Rev. Lett. **99**, 124502 (2007).
[6] M. Baron, J. Bławzdziewicz, and E. Wajnryb, Phys. Rev. Lett. **100**, 174502 (2008).
[7] H. Eral, D. van den Ende, F. Mugele, and M. Duits, Phys. Rev. E **80**, 061403 (2009).
[8] J. Blawzdziewicz, R. H. Goodman, N. Khurana, E. Wajnryb, and Y. N. Young, Physica D **239**, 1214 (2010).
[9] B. Cui, H. Diamant, and B. Lin, Phys. Rev. Lett. **89**, 188302 (2002).
[10] S. Navardi and S. Bhattacharya, Phys. Fluids **22**, 103306

(2010).
[11] S. Bhattacharya, J. Bławzdziewicz, and E. Wajnryb, J. Fluid Mech. **541**, 263 (2005).
[12] M. Zurita-Gotor, J. Bławzdziewicz, and E. Wajnryb, J. Fluid Mech. **592**, 447 (2007).
[13] G. Bossis, A. Meunier, and J. D. Sherwood, Phys. Fluids A **3**, 1853 (1991).
[14] See Supplemental Material at http://link.aps.org/ for movies, more on BMC method, collision model M3, interparticle potential, and the role of collision frequency.
[15] F. da Cunha and E. Hinch, J. Fluid Mech. **309**, 211 (1996).
[16] I. E. Zarraga and D. T. Leighton, Phys. Fluids **14**, 2194 (2002).
[17] D. R. Mikulencak and J. F. Morris, J. Fluid Mech. **520**, 215 (2004).
[18] J. M. Brader and M. Krueger, Mol. Phys. **109**, 1029 (2011).
[19] S. Cui, P. Cummings, and H. Cochran, J. Chem. Phys. **114**, 7189 (2001); A. Jabbarzadeh, P. Harrowell, and R. I. Tanner, Phys. Rev. Lett. **94** (2005).